Journal of Mechanics in Medicine and Biology
Vol. 15, No. 3 (2015) 1550023 (13 pages)

DOI: 10.1142/S0219519415500232

World Scientific
www.worldscientific.com

EXPERIMENTAL ASSESSMENT OF LUMPED-PARAMETER HUMAN BODY MODELS EXPOSED TO WHOLE BODY VIBRATION

YUNUS ZIYA ARSLAN

Department of Mechanical Engineering, Faculty of Engineering
Istanbul University, Avcilar, Istanbul, Turkey 34320
yzarslan@istanbul.edu.tr

Received 22 March 2014
Revised 17 July 2014
Accepted 31 July 2014
Published 23 September 2014

Whole body vibration (WBV) is uncontrolled vibrations in occupational settings such as vehicle driving or hand tool operating. Chronic occupational WBV exposure may cause many health problems such as fatigue, lower back pain, spinal degenerations, vision problems and so on. In order to simulate and observe the adverse effects of WBV on the human body, many lumped-parameter human body models were proposed. The objective of this study is to provide quantified assessments of human body biodynamic models which were designed to characterize the response of real human body exposed to WBV. To do so, direct measurements of vibration accelerations obtained from different segments of human body and vehicle seat were carried out during riding on roads with different unevenness levels. Recorded experimental acceleration data were compared with those obtained from simulations of different human body models. Root mean square difference and correlation coefficient values were calculated between theoretical and experimental accelerations for a quantitative assessment of the existing models. According to the comparison results, biodynamic model proposed by Boileau and Rakheja [Boileau P-É, Rakheja S, Whole-body vertical biodynamic response characteristics of the seated vehicle driver: Measurement and model development, *Int J Ind Ergonom* **22**:449–472, 1998] showed the best correlation with the experimental acceleration data.

Keywords: Human body biodynamic models; whole body vibration; vibration measurement.

1. Introduction

Whole body vibration (WBV) is the transmission of low frequency environmental vibration to the human body when in contact with the vibrating surface.[1] It is commonly experienced by drivers, operators and passengers in vehicles and machines when travelling over uneven surfaces. Long-term exposures to WBV may cause or exacerbate health problems such as respiratory, cardiovascular and digestive problems, reproductive organ damage, impairment of vision and balance, interference with activities and discomfort that could lead to accidents.[2–5] An

extensive review of epidemiologic studies reported that the occupational exposure to WBV is associated with an increased risk for low back pain, sciatic pain and lumbar intervertebral disc disorders.[6] The most common adverse effects induced by long-term exposure to WBV are low-back pain, early degeneration of the lumbar spinal system and herniated lumbar disc.[7] WBV also causes risk especially to the thoracic spine and the neck.[8]

The main sources of harmful WBV in vehicles are rough road and surface conditions. Since there is a high risk of damage to the human body while collecting vibration data including components that are causing mechanical damage to the human body, there is limited reliable information on such data.[9,10] Therefore, to evaluate and simulate the adverse effects of WBV to human body, many biodynamic lumped-parameter human body models were proposed (see Ref. 11 for an extensive review). Type of lumped-parameter model is relatively simple to analyze the dynamic behavior and easy to validate with empirical data. These models were developed in many studies to mainly observe the possible real human body responses to (i) different suspension designs and types of control algorithms in vehicles[12–15] and (ii) ergonomics of different seat designs.[16,17]

In this study, it was aimed to comparatively evaluate the characterization capabilities of widely used lumped parameter human body models which were developed to reflect the real human body responses to WBV.[18–20] To do so first, experimental vibration data of different segments of the human body exposed to WBV was recorded. Then, acceleration time histories of the human body models were obtained from simulation process and the theoretical results were quantitatively compared with the experimental results. The original contribution of this study is to provide a clear experimental assessment of the vibration acceleration responses of the human body models for repetitive trials under different road conditions.

2. Materials and Methods

2.1. *Human body models*

Lumped-parameter human body models are made up of several concentrated masses interconnected by springs and dampers.[11] In this study, acceleration responses of three widely used human biodynamic models were compared with direct vibration measurements. Hereafter, the model proposed by Wan and Schimmels,[18] Boileau and Rakheja[19] and Qassem *et al.*[20] are referred to as Model 1 (Fig. 1(a)), Model 2 (Fig. 1(b)) and Model 3 (Fig. 1(c)), respectively. Models 1 and 2 have 4 degrees of freedom (DoF) and Model 3 has 11 DoF.

In the figures, z_0 represents the displacement of the experimentally obtained disturbance coming from seat to human body. Displacement and mass of the body segments, coefficient of stiffness of the spring elements and coefficient of damping elements were denoted by z_i, m_i, k_i and c_i, respectively. To eliminate discrepancy

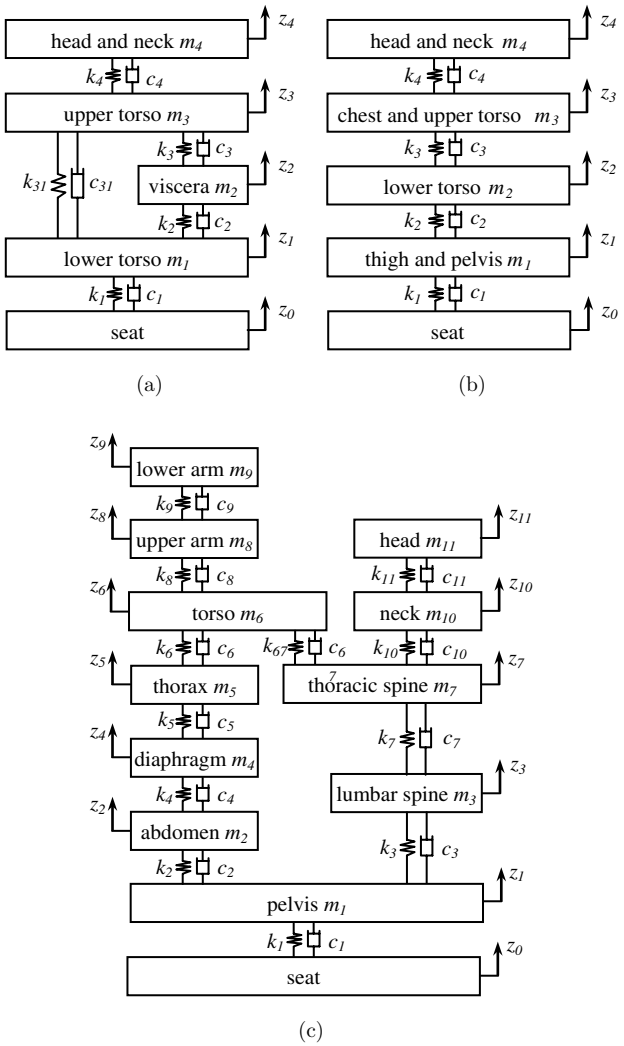

Fig. 1. Lumped-parameter models of human body compared in this study. (a) Model 1, (b) Model 2 and (c) Model 3.

between the mass of the subject and total mass of models, masses of body segments were scaled according to the mass of the subject. Equations of motion of the models were obtained using Lagranian approach. Equation of motions, along with the anthropometric and biomechanical data of all human body models, were given in Appendices A and B, respectively.

The only common body segments of all three models are head, upper torso and lower torso. In addition, these three parts of the human body are the most susceptible parts to the WBV.[4] Therefore, acceleration-time histories of these segments were analyzed in this study.

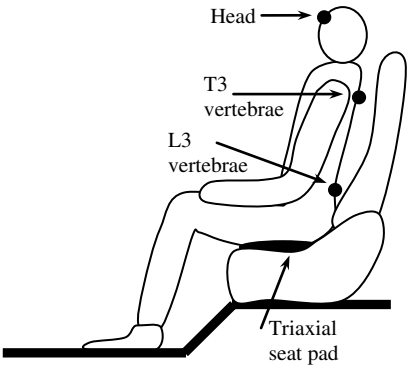

Fig. 2. Approximate positions of the accelerometers placed on the skin surface and vehicle seat.

2.2. *Experimental procedure*

In order to obtain direct measurements of WBV from different segments of human body and vehicle, the following experimental protocol was used.

In the measurement process, a 21 years-old male subject with 55 kg and without any chronic health disease was recruited. Uniaxial accelerometers (LMS SCADAS Mobile, Belgium) were placed onto the skin surface of head, upper torso (T3 vertebra) and lower torso (L3 vertebra) (Fig. 2) of the subject. In order to eliminate the change of positions of the sensors, these devices were temporarily fixed to the skin surface by means of bandages wrapped around the relevant body segments. Triaxial seat pad accelerometer was firmly fixed on the front-right seat of the vehicle using self-adhesive tape. The subject was asked to sit on the seat pad without backrest support. In addition to the subject, a driver and a technician, who sat on the rear-right seat and helped with the collection of the vibration signals into the computer, were also in the vehicle during vibration measurements.

In order to assess the effect of road unevenness on the characterization performance of the human body models, roads with three different types of pavement were chosen for the vibration measurements. The unevenness level of the first road was relatively high (Road 1), the second road had relatively middle roughness (Road 2) and the third road had relatively smooth surface (Road 3).

The speed of the vehicle was 30 km/h and vibration signals were collected for 64 s. Sampling rate of the signals was 512 Hz. In order to evaluate the consistency of the human model responses for repetitive trials, vibration measurement was repeated three times for each road profile. By doing so, acceleration responses of each lumped-parameter model were totally obtained for nine cases.

2.3. *Data analysis*

Direct measurements of vibration accelerations ($\ddot{z}_0$) transmitted from seat to human body were used as disturbance to all models. For all nine trials, acceleration-time responses of head, upper torso and lower torso were obtained in the simulation

process. Then these simulation results were compared with the experimental data which were collected from the relevant body segments.

In order to assess the difference between simulation and experimental acceleration data quantitatively, two error criteria were used, that is, root mean square difference (RMSD) and Pearson correlation coefficient (PCC).[21]

The RMSD between the experimental $a_{\text{exp}}(n)$ and theoretical $a_{\text{the}}(n)$ acceleration is calculated by the following equation

$$\text{RMSD} = \sqrt{\frac{\sum (a_{\text{exp}}(n) - a_{\text{the}}(n))^2}{\sum (a_{\text{exp}}(n))^2}}, \tag{1}$$

where n is the number of discrete signal data.

The value of RMSD gives the mean of percentage error, namely 0.05 means that the theoretical acceleration data has about 5% mean error from the experimental data.

PCC is a measure of the linear correlation (similarity) between two signals. It gives a value between +1 and −1, where +1 is total positive correlation, 0 is no correlation and −1 is total negative correlation. In our study, if the correlation coefficient is 0, then it is deduced that the theoretical and experimental accelerations are uncorrelated.

To observe whether the difference between average errors of human body models is statistical significant, one way ANOVA was used. The differences were evaluated at a level of significance of 0.01.

3. Results

Typical comparisons of experimental and theoretical vibration accelerations of Models 1, 2 and 3 for upper torso segment are shown in Fig. 3. The corresponding RMSD and PCC values are also given in the figure. It can be deduced from the figure that both RMSD and PCC are in agreement with the qualitative observation that the relatively lower RMSD and higher PCC values were calculated between similar experimental and theoretical signals.

RMSD and PCC values between theoretical and measured acceleration-time histories of the head, upper torso and lower torso segments were calculated for each trial and given in Tables 1, 2 and 3, respectively.

The average RMSD and PCC values were calculated for each human body model and given for head segment in Fig. 4, for upper torso segment in Fig. 5 and for lower torso segment in Fig. 6.

Model 1 gave the least RMSD errors for the head and lower torso (Figs. 4(a), 6(a)). However, Model 2 gave the least RMSD error for the upper torso (Fig. 5(b)). Also it was observed that all the best performances with respect to RMSD are statistically significant ($p < 0.01$). Model 3 showed a moderate characterization performance when compared with Models 1 and 2.

The highest PCC values were obtained from Model 2 for all investigated body segments, that is, best correlation with experimental data was obtained from the

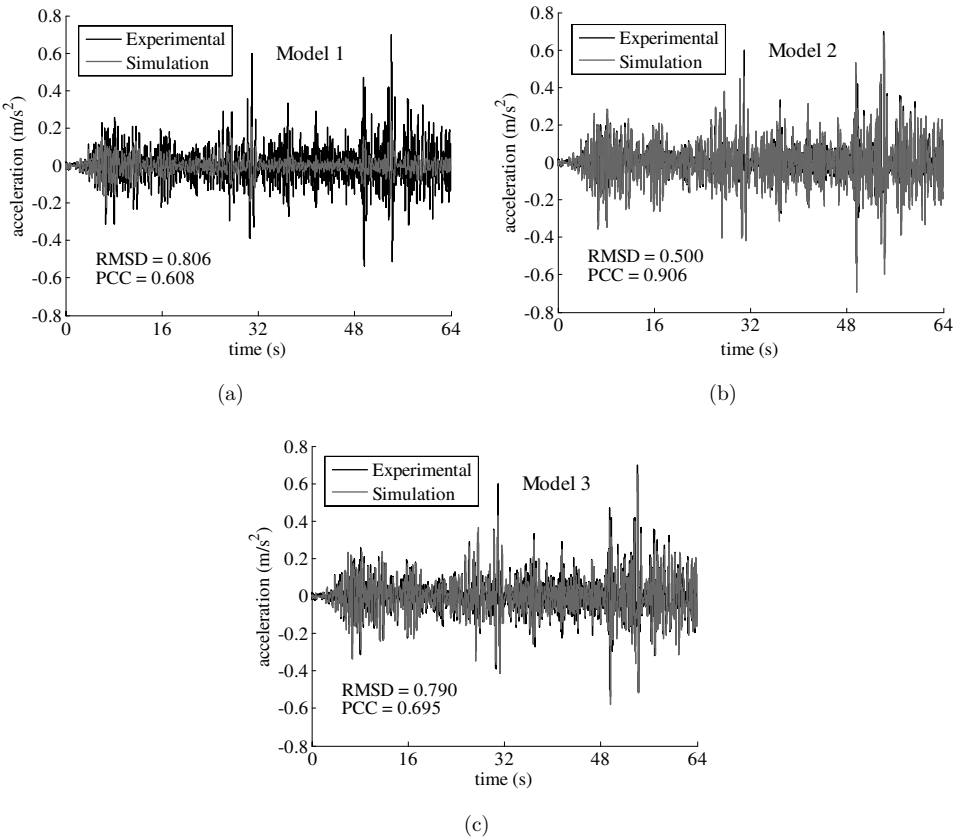

Fig. 3. Typical representation of experimental and theoretical acceleration-time responses obtained from (a) Model 1, (b) Model 2 and (c) Model 3, for upper torso.

Table 1. RMSD and correlation coefficient values between experimental and simulation results for head.

	Model 1		Model 2		Model 3	
Road profile and trial number	RMSD	Correlation coefficient	RMSD	Correlation coefficient	RMSD	Correlation coefficient
Road 1, trial 1	0.881	0.475	1.049	0.628	0.981	0.602
Road 1, trial 2	1.008	0.293	1.684	0.388	1.669	0.282
Road 1, trial 3	1.024	0.244	1.845	0.301	1.734	0.216
Road 2, trial 1	1.056	0.175	1.798	0.310	1.673	0.207
Road 2, trial 2	1.025	0.260	1.615	0.332	1.506	0.228
Road 2, trial 3	1.135	0.107	1.862	0.247	1.794	0.115
Road 3, trial 1	1.107	0.191	1.715	0.281	1.659	0.162
Road 3, trial 2	1.017	0.199	1.198	0.214	1.143	0.214
Road 3, trial 3	1.150	0.097	1.610	0.126	1.550	0.064

Table 2. RMSD and correlation coefficient values between experimental and simulation results for upper torso.

	Model 1		Model 2		Model 3	
Road profile and trial number	RMSD	Correlation coefficient	RMSD	Correlation coefficient	RMSD	Correlation coefficient
Road 1, trial 1	0.805	0.610	0.551	0.899	0.797	0.709
Road 1, trial 2	0.844	0.566	0.412	0.933	0.690	0.770
Road 1, trial 3	0.849	0.576	0.450	0.925	0.756	0.719
Road 2, trial 1	0.878	0.503	0.452	0.924	0.795	0.678
Road 2, trial 2	0.813	0.616	0.515	0.897	0.842	0.634
Road 2, trial 3	0.843	0.556	0.497	0.909	0.833	0.662
Road 3, trial 1	0.809	0.603	0.545	0.883	0.833	0.657
Road 3, trial 2	0.698	0.727	0.554	0.881	0.775	0.709
Road 3, trial 3	0.711	0.717	0.524	0.906	0.790	0.715

Table 3. RMSD and correlation coefficient values between experimental and simulation results for lower torso.

	Model 1		Model 2		Model 3	
Road profile and trial number	RMSD	Correlation coefficient	RMSD	Correlation coefficient	RMSD	Correlation coefficient
Road 1, trial 1	0.973	0.330	1.423	0.361	1.385	0.332
Road 1, trial 2	0.978	0.299	1.424	0.371	1.420	0.339
Road 1, trial 3	1.023	0.165	1.542	0.217	1.515	0.170
Road 2, trial 1	1.033	0.198	1.688	0.280	1.684	0.163
Road 2, trial 2	1.026	0.184	1.458	0.205	1.444	0.114
Road 2, trial 3	1.032	0.227	1.562	0.309	1.579	0.211
Road 3, trial 1	1.041	0.198	1.441	0.242	1.433	0.185
Road 3, trial 2	0.978	0.347	1.279	0.306	1.249	0.292
Road 3, trial 3	1.017	0.316	1.415	0.327	1.393	0.300

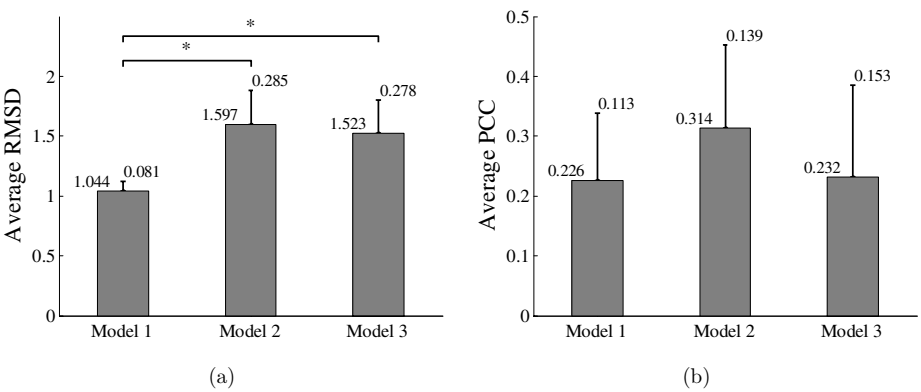

Fig. 4. Average (± standard deviation) values of (a) RMSD and (b) correlation coefficients between experimental and simulation results obtained for head. $*p < 0.01$.

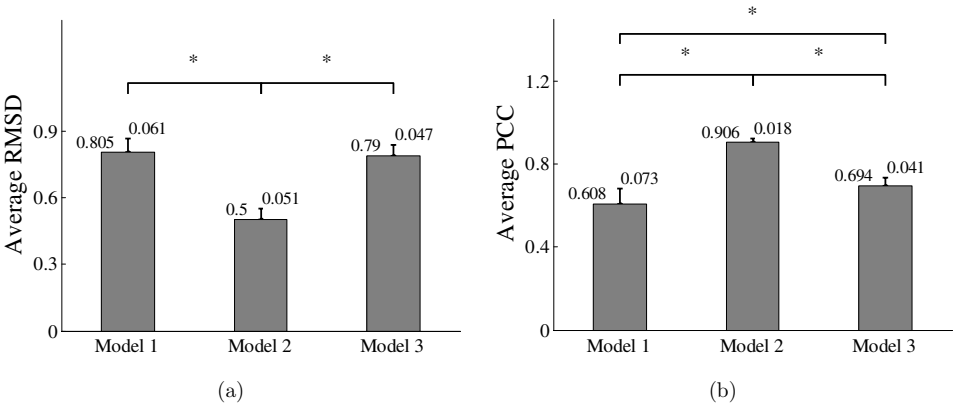

Fig. 5. Average (± standard deviation) values of (a) RMSD and (b) correlation coefficients between experimental and simulation results obtained for upper torso. $*p < 0.01$.

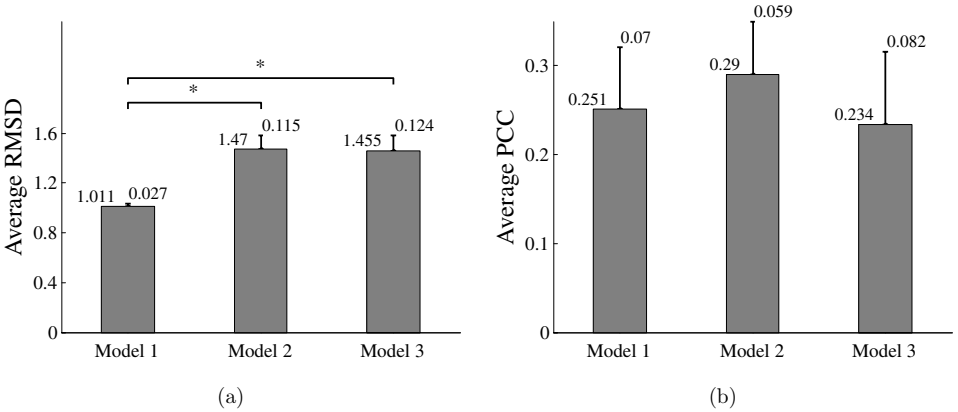

Fig. 6. Average (± standard deviation) values of (a) RMSD and (b) correlation coefficients between experimental and simulation results obtained for lower torso. $*p < 0.01$.

simulation results of Model 2. Moreover, for the upper torso segment, average PCC obtained from Model 2 is significantly higher than those obtained from Models 1 and 3.

4. Discussions

Measurement and assessment of WBV can be used to identify potentially damaging vibration levels exposing on drivers and workers, thereby enabling researchers to analyze the occupational health risks, ergonomics and comfort of vehicles and vehicle parts. However, vibration measurement is expensive and of high safety and health risks. Therefore, various human body models were proposed as indicators of responses of real human body to vibration exposures.[22,23]

As indicated by Nigam and Malik,[24] lumped parameter modeling of human body requires the following steps: (i) segmentation of the body into the concentrated masses, (ii) determination of mass, stiffness and damping parameters of segments and (iii) connecting the segments through spring and dashpot elements. All those steps directly require some assumptions to be made which results in divergence from the real human body behavior. Therefore, characterization of human body responses against disturbing effects using mathematical models is a challenging task.[23]

In this study, the characterization performances of the existing three human body models exposed to WBV in sitting position were comparatively evaluated. In terms of the RMSD values, best characterization performance was obtained from Model 1 for head and lower torso, from Model 2 for upper torso. If the PCC values are taken into account, best performance was obtained from Model 2 for all cases.

Best average RMSD and PCC values were obtained for upper torso segment from all three models, which indicates that the parameter identification of the models was better realized for the upper torso than two other segments.

A meaningful difference was not found between the average of RMSD and PCC values obtained for different road profiles. Therefore it can be deduced that unevenness level of the road profile does not affect the characterization performances of the models.

By taking the level of average errors obtained from all three models into account (Figs. 4, 5 and 6), it can be said that the existing human body models need refinements to reflect the biomechanical properties of the human body.[18–20]

The limitations of the study need to be noted. It is clear that not only the adverse effects of vibration on vehicle occupants stem from the vertical direction, but also horizontal vibrations cause side effects on human body. However, it is well accepted that major side effects associated with vehicle vibrations, such as spine fractures and intervertebral disc disorders are induced by strong vertical accelerations.[11] Therefore, the proposed human body models were constructed to analyze the effects of vertical vibrations, and this study used only the vertical component of the vibration data as disturbing effect coming from the road. Thus, the subject was asked to sit in an upright position without backrest support during measurement process, even if this position is not the usual during riding. Another limitation of the study is the speed of the vehicle which is a low value for car driving. The measurement of vibrations was performed on roads with three different unevenness levels and it was aimed to compare the effects of different road profiles on human body models under same conditions, such as same riding duration, same vehicle speed and same number of trials. The unevenness level of the Road 1 was relatively high, hence if the speed of the vehicle was higher than the predefined value of 30 km/h, it would result in high level of vibration displacements and might lead to a risky measurement protocol for the vehicle occupants. Therefore, to be able to use the same vehicle speed for all road types, a relatively low speed of vehicle was determined in the study. Furthermore, to see if the characterization features of the human body models are sensitive to the different road conditions and consistent within the repetitive trials, it was

considered to provide a clear and simple comparison of the human body models. Therefore, data collection was performed from only one subject, but for repetitive trials under different road conditions. However, to find out if the vibration acceleration responses of the different parts of the real human body are sensitive to the subject factors such as age, gender and physical conditions and if the human body models accurately reflect the vibration responses of a diverse subject group, it is required to collect the data from more subjects with different physical properties.

5. Conclusions

Due to the safety and health risks and hazardous environments, it is nearly impossible to recruit real human subjects to collect vibration data including damaging components to human body. Thus, obtaining reliable simulation results from human body models, which are aimed to characterize the real human behavior, is of high importance. It can be concluded from this study that human biodynamic model proposed by Boileau and Rakheja[19] gave the best acceleration-time response correlation with the experimental data. Moreover, the least RMSD error was found using the model proposed by Wan and Schimmels[18] for the head and lower torso segments. None of the models best fitted to all cases. Therefore, these models require optimum parameter identification analysis for the best characterization capability of the real human body, which is intended to be the further step of this research.

Acknowledgments

This research was supported by The Research Fund of the Istanbul University, Project No. UDP-43716 and YADOP-42672.

References

1. Griffin MJ, *Handbook of Human Vibration*, Academic Press, London, 1990.
2. Johanning E, Back disorders and health problems among subway train operators exposed to whole-body vibration, *Scand J Work Environ Health* **17**:414–419, 1991.
3. Paddan GS, Griffin MJ, A review of the transmission of translational seat vibration to the head, *J Sound Vib* **215**:863–882, 1998.
4. Lings S, Leboeuf-Yde C, Whole-body vibration and low back pain: A systematic, critical review of the epidemiological literature 1992–1999, *Int Arch Occ Env Hea* **73**:290–297, 2000.
5. Cardinale M, Pope MH, The effects of whole body vibration on humans: Dangerous or advantageous? *Acta Physiol Hung* **90**:195–206, 2003.
6. Hulshof C, van Zanten BV, Whole-body vibration and low-back pain, *Int Arch Occ Env Hea* **59**:205–220, 1987.
7. Bovenzi M, Hulshof CT, An updated review of epidemiologic studies on the relationship between exposure to whole-body vibration and low back pain (1986–1997), *Int Arch Occ Env Hea* **72**:351–365, 1999.
8. Seidel H, On the Relationship between whole-body vibration exposure and spinal health risk, *Ind Health* **43**:361–377, 2005.

9. von Gierke HE, Brammer AJ, Effects of shock and vibration on humans, in Harris CM, Piersol AG (eds.), *Harris' Shock and Vibration Handbook*, 5th edn., McGraw Hill, New York, pp. 42.1–42.62, 2002.
10. Afkar A, Javanshir I, Ahmadian MT, Ahmadi H, Optimization of a passenger occupied seat with suspension system exposed to vertical vibrations using genetic algorithms, *J Vibroeng* **15**:979–991, 2013.
11. Liang CC, Chiang CF, A study on biodynamic models of seated human subjects exposed to vertical vibration, *Int J Ind Ergonom* **36**:869–890, 2006.
12. Han YM, Jung JY, Choi SB, Wereley NM, Sliding model control of ER seat suspension considering human vibration model, *Int J Mod Phys B* **19**:1689–1695, 2005.
13. Sezgin A, Arslan YZ, Analysis of the vertical vibration effects on ride comfort of vehicle driver, *J Vibroeng* **14**:559–571, 2012.
14. Du H, Li W, Zhang N, Vibration control of vehicle seat integrating with chassis suspension and driver body model, *Adv Struct Eng* **16**:1–9, 2013.
15. Arslan YZ, Sezgin A, Yagiz N, Improving the ride comfort of vehicle passenger using fuzzy sliding mode controller, to appear in *J Vib Control*, doi: 10.1177/1077546313500061.
16. Cho Y, Yoon YS, Biomechanical model of human on seat with backrest for evaluating ride quality, *Int J Ind Ergonom* **27**:331–345, 2001.
17. Rakheja S, Afework Y, Sankar S, An analytical and experimental investigation of the driver-seat-suspension system, *Vehicle Syst Dyn* **23**:1513–1531, 1994.
18. Wan Y, Schimmels JM, A simple model that captures the essential dynamics of a seated human exposed to whole body vibration, *Bioeng Div ASME* **31**:333–334, 1995.
19. Boileau P-É, Rakheja S, Whole-body vertical biodynamic response characteristics of the seated vehicle driver: Measurement and model development, *Int J Ind Ergonom* **22**:449–472, 1998.
20. Qassem W, Othman MO, Abdul-Majeed S, The effects of vertical and horizontal vibrations on the human body, *Med Eng Phys* **16**:151–161, 1994.
21. Arslan YZ, Jinha A, Kaya M, Herzog W, Prediction of muscle forces using static optimization for different contractile conditions, *J Mech Med Biol* **13**:1–13, 2013.
22. Marzbanrad J, Afkar A, A biomechanical model as a seated human body for calculation of vertical vibration transmissibility using a genetic algorithm, *J Mech Med Biol* **13**:1–18, 2013.
23. Liang CC, Chiang CF, Modeling of a seated human body exposed to vertical vibrations in various automotive postures, *Ind Health* **46**:125–137, 2008.
24. Nigam SP, Malik M, A study on a vibratory model of a human body, *J Biomech Eng* **109**:148–153, 1987.

Appendix A
Equations of motion of Model 1

$$m_1\ddot{z}_1 + c_1(\dot{z}_1 - \dot{z}_0) + c_2(\dot{z}_1 - \dot{z}_2) + c_{31}(\dot{z}_1 - \dot{z}_3) + k_1(z_1 - z_0) + k_2(z_1 - z_2) + k_{31}(z_1 - z_3) = 0, \tag{A.1}$$

$$m_2\ddot{z}_2 + c_2(\dot{z}_2 - \dot{z}_1) + c_3(\dot{z}_2 - \dot{z}_3) + k_2(z_2 - z_1) + k_3(z_2 - z_3) = 0, \tag{A.2}$$

$$m_3\ddot{z}_3 + c_3(\dot{z}_3 - \dot{z}_2) + c_{31}(\dot{z}_3 - \dot{z}_1) + c_4(\dot{z}_3 - \dot{z}_4) + k_3(z_3 - z_2) + k_{31}(z_3 - z_1) + k_4(z_3 - z_4) = 0, \tag{A.3}$$

$$m_4\ddot{z}_4 + c_4(\dot{z}_4 - \dot{z}_3) + k_4(z_4 - z_3) = 0. \tag{A.4}$$

Equations of motion of Model 2

$$m_1\ddot{z}_1 + c_1(\dot{z}_1 - \dot{z}_0) + c_2(\dot{z}_1 - \dot{z}_2) + k_1(z_1 - z_0) + k_2(z_1 - z_2) = 0, \quad \text{(A.5)}$$

$$m_2\ddot{z}_2 + c_2(\dot{z}_2 - \dot{z}_1) + c_3(\dot{z}_2 - \dot{z}_3) + k_2(z_2 - z_1) + k_3(z_2 - z_3) = 0, \quad \text{(A.6)}$$

$$m_3\ddot{z}_3 + c_3(\dot{z}_3 - \dot{z}_2) + c_4(\dot{z}_3 - \dot{z}_4) + k_3(z_3 - z_2) + k_4(z_3 - z_4) = 0, \quad \text{(A.7)}$$

$$m_4\ddot{z}_4 + c_4(\dot{z}_4 - \dot{z}_3) + k_4(z_4 - z_3) = 0. \quad \text{(A.8)}$$

Equations of motion of Model 3

$$m_1\ddot{z}_1 + c_1(\dot{z}_1 - \dot{z}_0) + c_2(\dot{z}_1 - \dot{z}_2) + c_3(\dot{z}_1 - \dot{z}_3) + k_1(z_1 - z_0) + k_2(z_1 - z_2) + k_3(z_1 - z_3) = 0, \quad \text{(A.9)}$$

$$m_2\ddot{z}_2 + c_2(\dot{z}_2 - \dot{z}_1) + c_4(\dot{z}_2 - \dot{z}_4) + k_2(z_2 - z_1) + k_4(z_2 - z_4) = 0, \quad \text{(A.10)}$$

$$m_3\ddot{z}_3 + c_3(\dot{z}_3 - \dot{z}_1) + c_7(\dot{z}_3 - \dot{z}_7) + k_3(z_3 - z_1) + k_7(z_3 - z_7) = 0, \quad \text{(A.11)}$$

$$m_4\ddot{z}_4 + c_4(\dot{z}_4 - \dot{z}_2) + c_5(\dot{z}_4 - \dot{z}_5) + k_4(z_4 - z_2) + k_5(z_4 - z_5) = 0, \quad \text{(A.12)}$$

$$m_5\ddot{z}_5 + c_5(\dot{z}_5 - \dot{z}_4) + c_6(\dot{z}_5 - \dot{z}_6) + k_5(z_5 - z_4) + k_6(z_5 - z_6) = 0, \quad \text{(A.13)}$$

$$m_6\ddot{z}_6 + c_6(\dot{z}_6 - \dot{z}_5) + c_{67}(\dot{z}_6 - \dot{z}_7) + c_8(\dot{z}_6 - \dot{z}_8) + k_6(z_6 - z_5) + k_{67}(z_6 - z_7) + k_8(z_6 - z_8) = 0, \quad \text{(A.14)}$$

$$m_7\ddot{z}_7 + c_{67}(\dot{z}_7 - \dot{z}_6) + c_7(\dot{z}_7 - \dot{z}_3) + c_{10}(\dot{z}_7 - \dot{z}_{10}) + k_{67}(z_7 - z_6) + k_7(z_7 - z_3) + k_{10}(z_7 - z_{10}) = 0, \quad \text{(A.15)}$$

$$m_8\ddot{z}_8 + c_8(\dot{z}_8 - \dot{z}_6) + c_9(\dot{z}_8 - \dot{z}_9) + k_8(z_8 - z_6) + k_9(z_8 - z_9) = 0, \quad \text{(A.16)}$$

$$m_9\ddot{z}_9 + c_9(\dot{z}_9 - \dot{z}_8) + k_9(z_9 - z_8) = 0, \quad \text{(A.17)}$$

$$m_{10}\ddot{z}_{10} + c_{10}(\dot{z}_{10} - \dot{z}_7) + c_{11}(\dot{z}_{10} - \dot{z}_{11}) + k_{10}(z_{10} - z_7) + k_{11}(z_{10} - z_{11}) = 0, \quad \text{(A.18)}$$

$$m_{11}\ddot{z}_{11} + c_{11}(\dot{z}_{11} - \dot{z}_{10}) + k_{11}(z_{11} - z_{10}) = 0. \quad \text{(A.19)}$$

Appendix B. Model Parameters

Table B.1. Numerical values of the parameters of Model 1.

Mass (kg)	Stiffness (N/m)	Damping (Ns/m)
m_1:32.635	k_1:49340	c_1:2475
m_2:4.985	k_2:20000	c_2:330
m_3:13.598	k_3:10000	c_3:200
m_4:3.780	k_{31}:192000	c_{31}:909.1
	k_4:134400	c_4:250

Table B.2. Numerical values of the parameters of Model 2.

Mass (kg)	Stiffness (N/m)	Damping (Ns/m)
m_1:12.733	k_1:90000	c_1:2064
m_2:8.588	k_2:162800	c_2:4548
m_3:28.386	k_3:183000	c_3:4750
m_4:5.290	k_4:310000	c_4:400

Table B.3. Numerical values of the parameters of Model 3.

Mass (kg)	Stiffness (N/m)	Damping (Ns/m)
m_1:16.332	k_1:25016	c_1:370.8
m_2:3.542	k_2:877	c_2:292.3
m_3:1.200	k_3:52621	c_3:3581.6
m_4:0.272	k_4:877	c_4:292.3
m_5:0.816	k_5:877	c_5:292.3
m_6:19.611	k_6:52621	c_6:3581.6
m_7:2.882	k_{67}:877	c_{67}:292.3
m_8:3.280	k_7:52621	c_7:3581.6
m_9:3.177	k_8:67542	c_8:3581.6
m_{10}:0.650	k_9:67542	c_9:3581.6
m_{11}:3.265	k_{10}:52621	c_{10}:3581.6
	k_{11}:52621	c_{11}:3581.6